J. Marine. Sci. Appl. (2010) 9: 163-167
DOI: 10.1007/s11804-010-9027-7

Modeling Loads Caused by Breaking Waves Striking Vertical Walls

Hai-gui Kang* **and Ying-wei Sun**

State Key Laboratory of Coastal & Offshore Engineering, Dalian University of Technology, Dalian 116024, China

Abstract: Breaking waves can have tremendous destructive impact on vertical walls, yet they are poorly understood. By using particle imaging velocimetry (PIV) technology and high-precision pressure transducers, actual breaking wave loads on vertical walls were studied. By simultaneously comparing the flow field structure and wave pressure, the mechanisms of breaking wave pressure could be analyzed. The probability distribution of the peak value of the first impact of a breaking wave was investigated. The results showed that the impact pressure p is mainly distributed in the range of 0.25-2.75 ρv^2, with the greatest possible probability at $p/\rho v^2 = 0.75$.

Keywords: vertical breakwater; breaking wave; wave loads; particle imaging velocimetry (PIV)
Article ID: 1671-9433(2010)02-0163-05

1 Introduction

Vertical walls are one of the most common structures in ocean engineering. When compared with standing waves, breaking waves have been found to have tremendous destructive impact on vertical walls. Since the 1950s, a lot of research on breaking waves has been done and many hypotheses for calculating breaking wave pressure, such as Jet Theory, Air Cushion Theory(Minikin, 1950), Water Momentum Theory and Water Hammer theory, have been proposed. In China, a systematic study of breaking wave pressure (Hou and LI, 1974; Liu, 1985) was carried out in Dalian University of Technology, and a method for calculating the breaking wave pressure under regular wave condition was proposed (Sea Code Group, 1974; Li *et al*., 1997). The breaking wave flow field has significant influence on wave pressure. But until now, most of the studies about breaking waves are focused on the wave pressure and little research works on flow fields has been done. So the relationship between the wave's pressure field and flow field is unclear.

In this study, the wave pressures and water particles velocity of breaking wave which is under high mound condition are sampled synchronously by using PIV system. By contrasting the flow field structure and the wave pressure, the characteristics of breaking wave flow field and pressure field are explored. The relationship between water particles velocity and wave pressures is analyzed with probability method.

Received date: 2009-05-06.
Foundation item: Supported by the National Natural Science Foundation of China under Grant No.50679008.
***Corresponding author Email:** hgkang@dlut.edu.cn

2 Physical model test

2.1 Experimental facilities

The experiment was carried out in the PIV wave flume at the State Key Laboratory of Coastal and Offshore Engineering, Dalian University of Technology.

2.1.1 Wave flume

The flume is 24 meters long, 0.45 meters wide and 0.6 meters deep. It is equipped with a wave maker driven by a servo-electro-hydraulic system, a related computer control and data acquisition system.

2.1.2 PIV system

(1) Two Laser Generators were used as the illuminator, which were placed under the wave tank to illuminate upwards vertically and controlled by a computer to provide a thin light sheet.

(2) A high speed Powerview CCD Camera produced by TSI in USA allows the real time capture of two image sequences, 512×512 resolution at 262 fps.

(3) Coreco Camera link Image Acquisition Card and LaserPulse Synchronizer were used to control the image sampling and the synchronization of CCD camera and laser generator.

(4) The PVC powder of 150 μm grain size was used as tracer particles.

(5) The Insight^{TM}3G software was applied for the image processing, analysis, and measurement operations.

2.1.3 Wave gauges and wave force pressure transducers

The wave gauge was used to calibrate the input wave height

and would be removed in the formal test. The sampling frequency of wave pressure transducer was 500Hz.

2.2 Experimental conditions

The wave parameters and test conditions are shown in Table 1, in which H is wave height, T is wave period, d is water depth, d_1 is the water depth on the mound.

2.3 Experimental method

2.3.1 Model

The breakwater model was made of plexiglass of 44cm long, 40cm wide and 45cm high. The width of toe berm was 15cm. The experimental setup is shown in Fig.1.

Table 1 Wave parameters and test conditions

Section	H / cm	T / s	d / cm	d_1 / cm
1	9	1	30	9
2			35	
3	10	1.1	30	9
4			35	
5	11	1.2	30	9
6			35	

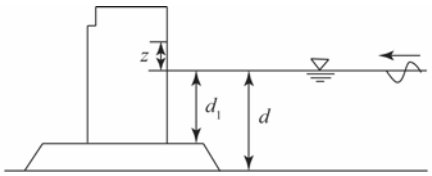

Fig.1 Plan view of experimental setup

2.3.2 Experimental procedures

The breakwater and mound models were installed in the PIV wave flume. Five pressure transducers were fixed on one side of the vertical walls, and were marked as 1 to 5 starting from the bottom, as shown in Fig.2.

The frame rate of CCD camera was 200HZ, and the time interval between two frames was 5 ms. The pressure sampling synchronized with the image sampling at the same interval. For each test condition, a series of images were recorded in successive instants by the PIV system and the time series of wave force pressure were recorded by the pressure transducers simultaneously.

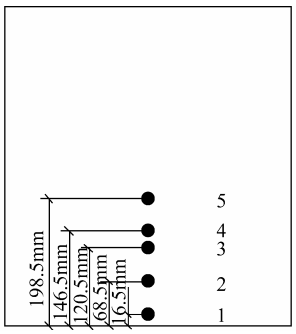

Fig.2 Sketch of pressure transducers on the breakwater model

3 Analysis of experimental result

InsightTM3G software was used to analyze the PIV images. In the processing of data, classic Nyquist grid and Fast Fourier Transform method were adopted to perform cross-correlation analysis for the double-exposure images. Vector analysis software package was also used to reduce the error in result.

3.1 Impact process of breaking wave

Velocity fields of a half cycle of breaking wave impacting on the vertical wall are given in Fig.5, in which the horizontal and vertical coordinates are the distances of respective direction, gray vertical line is the vertical wall.

Quite different from the spilling breaking under the medium-height mound condition (Kang *et al*., 2008), plunging breaking would occur under the high mound condition. By contrasting the instantaneous velocity fields and wave pressure fields of various instants shown in Fig.3 and Fig.4, it can be seen that at the instant t=0, wave crest moves to the top of the mound and curls, so plunging breaking occurs. The wave pressures of transducers 2, 3 and 4, whose location are higher than the water level, are zero, transducer 1 is under water and its wave pressure is negative.

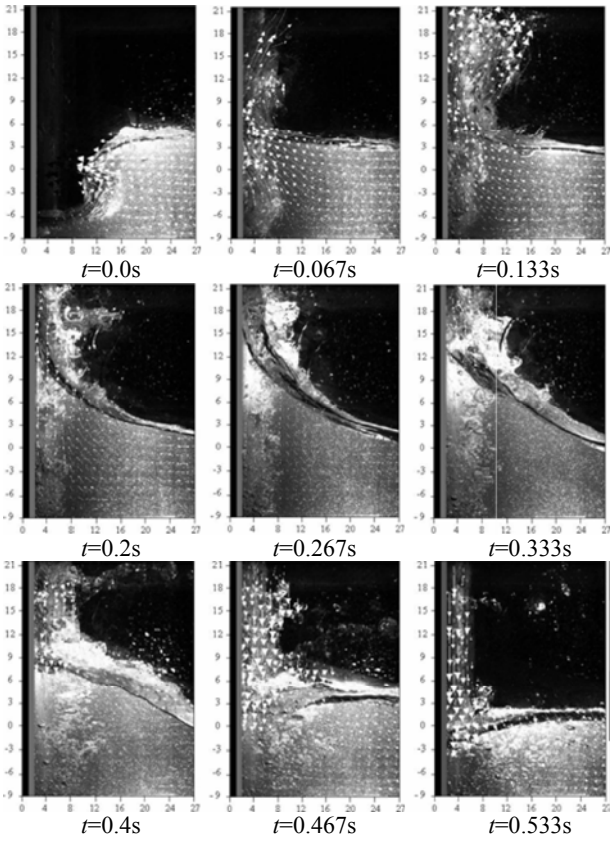

(High mound, H=10cm, T=1.1s)

Fig.3 The instantaneous fluid fields

At the instant t=0.067s, the formed water tongue has already impacted on the wall directly and strongly. The wave pressure of transducers 1 and 2 increases rapidly and reaches the biggest value at 0.033s. Obviously, the impact energy of the water tongue causes the first peak value of wave pressure. The PIV image at t=0s shows that transducers 1 and 2 are in the impact area of the water tongue and transducers 3 and 4 are outside that area. So it is easy to explain why the wave pressure of transducers 3 and 4 is nearly to zero at the impact instant. At the instant t=0.133s, the water surface is climbing up along the wall continuously and the wave pressure on the wall is getting down gradually. From the instant t=0.2 s to 0.267 s, the water surface is climbing up along the wall continuously and quickly, and the wave pressure on the wall is getting down. At the instant t=0.333 s, the water surface reaches the highest point along the wall. The wave pressure reaches the second peak value at t=0.36 s. After that, the water surface and wave pressure are getting down gradually. At the instant t=0.533 s, the water surface is getting to SWL (stationary water level) and the wave pressure is getting to zero.

Due to the impact of water tongue, the first peak value of wave pressure has a large intensity and lasts a very short time. The temporal curve of the first peak value is in triangular shape. Obviously, the impact wave force measured by transducers 1 and 2 has a great contribution to the total wave force.

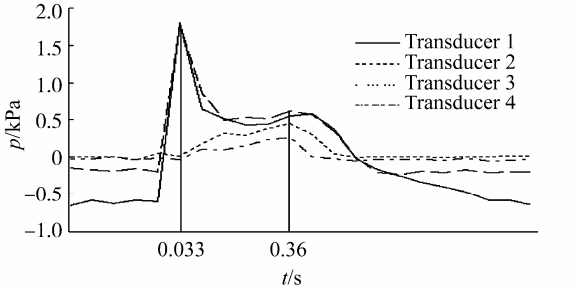

(High mound, H=10 cm, T=1.1s, d=30 cm)

Fig.4 The temporal curves of wave pressure

3.2 First peak pressure value analysis

The above analysis shows that the first peak value of wave pressure with triangular distribution is caused by the impact of water tongue formed in the wave breaking process and closely related to the impact velocity, which is defined as the average velocity (in horizontal direction) of the water particles from the water tongue at the moment of the tongue impacting on the vertical breakwater. The velocities of these water particles are sampled at different locations of the water tongue. From PIV images (Fig.5), it can be seen that the wave breaking process is very complicated, and the extent of plunging breaking has a random property. So, the impact velocity is very different from each impact process. This is also the reason why the first peak value of wave pressure has the random property. Fig.6 is the temporal curve of wave pressure synchronized with Fig.5. It clearly shows the random property of the first peak pressure of wave.

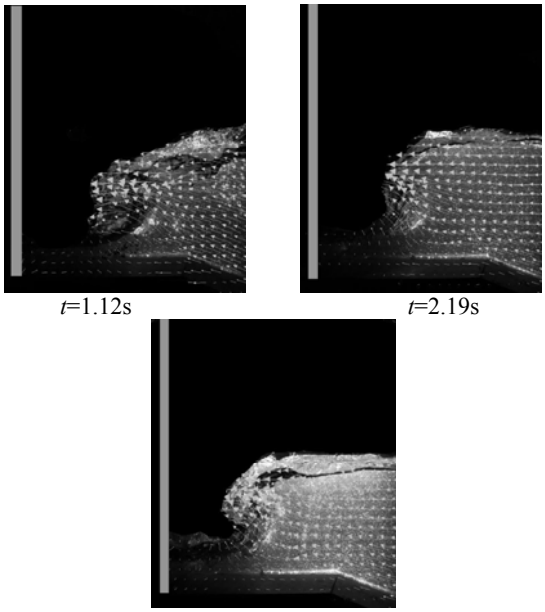

(High mound, H=10 cm, T=1.1 s, d=30 cm)

Fig.5 Different instants before wave impacting on the wall

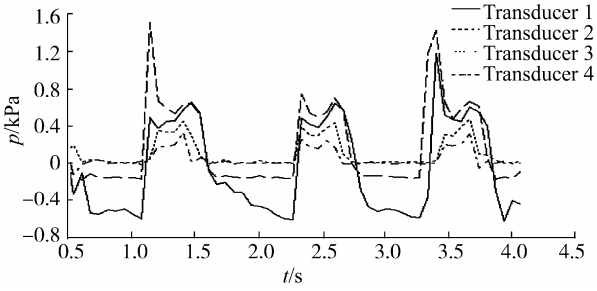

(High mound, H=10 cm, T=1.1s, d=30 cm)

Fig.6 The temporal curves of wave pressure

A statistical analysis is given to the dimensionless parameter $p/\rho v^2$, in which p is the first peak pressure value and v is the impact velocity of the water particles synchronized with the wave pressure. Fig.7 is the histogram of statistical probability distribution of $p/\rho v^2$. It can be seen that the values of $p/\rho v^2$ are very discrete and the distribution range is between 0.25~7. The most probable value of $p/\rho v^2$ is 0.75. The probability of $p/\rho v^2$ between 0.25~2.75 is 0.85. In other words, for most cases, the wave pressure is about 0.25~2.75 $p/\rho v^2$ at the instant of impact. The exact relationship between impact velocity and impact wave pressure is expected to be found out with a further work.

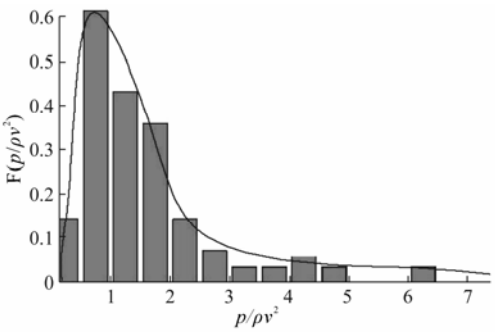

Fig.7 Histogram of statistical probability distribution of $p/\rho v^2$

Table 2 Comparison between first and second peak value (High mound, H=10 cm, T=1.1 s, d=30 cm) kPa

Impact process	Transducer 2 peak value		Transducer 2 peak value		Transducer 3 peak value		Transducer 4 peak value	
	1st	2nd	1st	2nd	1st	2nd	1st	2nd
1	1.175	0.624	0.923	0.684	1.322	0.403	1.283	0.184
2	1.865	0.64	1.91	0.643	0.512	0.495	0.176	0.34
3	0.975	0.674	1.574	0.651	0.808	0.495	0.807	0.25
4	0.674	0.64	0.791	0.709	0.512	0.521	0.225	0.307
5	0.567	0.575	0.887	0.632	0.645	0.442	0.301	0.26
6	0.483	0.642	1.505	0.689	0.341	0.425	0.178	0.317
7	0.475	0.634	0.747	0.648	0.383	0.459	0.252	0.235
8	1.169	0.592	1.422	0.65	0.299	0.43	0.194	0.309
9	1.49	0.712	1.578	0.672	1.076	0.427	0.755	0.255
10	0.487	0.604	0.746	0.688	0.275	0.469	0.255	0.263
11	2	0.62	1.78	0.614	0.393	0.419	0.247	0.296
12	1.515	0.646	3.644	0.68	0.494	0.427	0.222	0.288

3.3 Second peak pressure value analysis

Fig. 6 and Table 2 show that, the second peak value of wave pressure is much more stable than the first peak value. It means that the first peak value almost has no influence on the second peak value. In other words, the breaking process doesn't influence the second peak value greatly.

For the first peak value, the relationship between p_b (wave pressure at bottom) and p_s (wave pressure at still water level) can be described as p_b=0.6p_s (Code of Hydrology for Sea Harbour, China). But the second peak pressure doesn't satisfy this equation. From Table 3, it can be found that the value of p_b is very close to the value of p_s , and p_b/p_s is between 0.86~0.99.

The wave forces resulting from the second peak value of wave pressures are not expected to cause any serious damage to coastal structures (Kirkgoz, 1995), so there is no further analysis of the relationship between the second peak pressure values and flow fields.

Table 3 The second wave pressure at different locations

Item	p /kPa	H=9 cm	H=10 cm	H=11 cm
d =30 cm d_1=9 cm	p_s	0.567	0.673	0.776
	p_b	0.486	0.634	0.764
d =35 cm d_1=9 cm	p_s	0.57	0.68	0.81
	p_b	0.5	0.67	0.79

4 Conclusions

By contrasting the flow field structures and the wave pressures synchronously, the mechanism of breaking wave pressure on vertical walls under high mound condition is discussed, and the following conclusions can be obtained:

1) The distribution forms of wave pressure curves and the wave breaking types are closely related. Different from the spilling breaking type which happens under the medium-height mound condition, the wave breaks in the plunging breaking type under high mound condition. The wave pressure curve has a triangular shape with a large intensity and the wave forces on walls last a very short time.

2) The triangular distribution of wave pressure is caused by the impact of water tongue formed in the breaking process and has a great contribution to the total wave force. The distribution of the first peak value is closely related to the impact velocity of the water tongue. The greatest possible probability is at $p/\rho v^2$ = 0.75. For most cases, the impact pressure p is mainly distributed in the range of 0.25-2.75 ρv^2.

3) The breaking process doesn't influence the second peak value (in both of the two distribution forms) of wave pressure very much. The second peak value is much more stable than the first peak value, and p_b/p_s is between 0.86~0.99.

References

Hou MT, Li YC (1963). Interaction between wave and vertical breakwater. *Journal of Dalian University of Technology*, 3, 1-28.

Kang HG, Sun, YW, Qu XT (2008). Study on mechanism of breaking wave loads on vertical walls. *Chinese-German Joint Symposium on Hydraulic and Ocean Engineering*, Darmstadt, 433-438.

Kirkgoz MS (1995). Breaking wave impact on vertical and sloping coastal structures. *Ocean Engineering,* **22**(1), 45-48.

Kirkgoz MS, Akoz MS (2005). Geometrical properties of perfect breaking waves on composite breakwaters. *Ocean Engineering*, **32**, 1994-2006.

Li YC, Liu DZ, Su XJ, Qi GP (1997). The irregular wave force on vertical walls. *Journal of dynamics,* **12**(4), 456-469.

Li YC, Teng B (2002). *Wave Action on Maritime Structures*. China Ocean Press, Beijing, 178-191.

Liu DZ (1985). Discussion on the formula of breaking wave loads calculation. *Coastal Engineering*, **4**(2), 11-20.

Minikin RR (1950). *Wind Waves and Maritime Structures*. New York, US, 99-101.

Ren B, Li XL, Wang YX (2006). Experimental investigation of instantaneous properties of the flow field of wave slamming. *Ocean Engineering,* **24**(4), 68-74.

Research group for code of sea port in Dalian University of Technology (1975). Breaking wave force. *Journal of Dalian University of Technology*, 81-104.

Serio FD, Mossa M (2006). Experimental study on the hydrodynamics of regular breaking waves. *Coastal Engineering*, **53**, 99-113.

Sun HQ, Kang HG, Li GW (2002). Theory and application of PIV. *Journal of Waterway and Harbour*, **23**(1), 42-45.

Hai-gui Kang was born in 1945. He is the professor of Dalian University of Technology. His current research interests include coastal defence engineering, ocean engineering, *etc*.

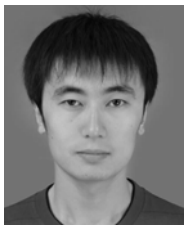

Ying-wei Sun was born in 1981. He is the PHD candidate in the Dalian University of Technology. His research fields include numerical simulation of ocean waves, evaluation of marine energy, *etc*.

The 20th International Offshore (Ocean) and Polar Engineering Conference & Exhibition (ISOPE 2010)

June 20-26, 2010, Beijing, China

The ISOPE, the International Society of Offshore and Polar Engineers, was granted on September 15, 1989 the status of tax-exempt, non-profit scientific and educational organization under Code 501(c)(3) from the United States Internal Revenue Code. The ISOPE opened its offices initially in the USA, the UK and Norway. The Society membership is open equally to all actively interested in promoting engineering and scientific progress in the fields of offshore and polar engineering. The membership comes initially from more than 30 countries, and encompasses a variety of activities including technical conferences, publications, scholarship and professional recognition programs, continuing education, and international cooperation. The Society's annual conference, the Annual International Offshore and Polar Engineering Conference, is one of the world's largest of its kind with refereed papers. The conference has been held alternatively among the continents, and has had participants from more than 50 countries.

The primary objectives of the Society are:

- to advance at an international level the arts and sciences in and promote and improve technological progress in the interdisciplinary fields of offshore, ocean and polar engineering and related technologies through international cooperation and participation;
- to disseminate scientific knowledge and provide timely exchange of technical knowledge and information;
- to provide opportunities through its programs for interested individuals to maintain and improve their individual technical competence in these fields, for the benefit of the public and the interested engineers in these fields.